

# Cancer Research

## The SmoA1 Mouse Model Reveals That Notch Signaling Is Critical for the Growth and Survival of Sonic Hedgehog-Induced Medulloblastomas

Andrew R. Hallahan, Joel I. Pritchard, Stacey Hansen, et al.

*Cancer Res* 2004;64:7794-7800. Published online November 1, 2004.

**Updated Version**

Access the most recent version of this article at:  
doi:[10.1158/0008-5472.CAN-04-1813](https://doi.org/10.1158/0008-5472.CAN-04-1813)

**Supplementary Material**

Access the most recent supplemental material at:  
<http://cancerres.aacrjournals.org/content/suppl/2004/11/11/64.21.7794.DC1.html>

**Cited Articles**

This article cites 48 articles, 21 of which you can access for free at:  
<http://cancerres.aacrjournals.org/content/64/21/7794.full.html#ref-list-1>

**Citing Articles**

This article has been cited by 59 HighWire-hosted articles. Access the articles at:  
<http://cancerres.aacrjournals.org/content/64/21/7794.full.html#related-urls>

**E-mail alerts**

[Sign up to receive free email-alerts](#) related to this article or journal.

**Reprints and Subscriptions**

To order reprints of this article or to subscribe to the journal, contact the AACR Publications Department at [pubs@aacr.org](mailto:pubs@aacr.org).

**Permissions**

To request permission to re-use all or part of this article, contact the AACR Publications Department at [permissions@aacr.org](mailto:permissions@aacr.org).

# The SmoA1 Mouse Model Reveals That Notch Signaling Is Critical for the Growth and Survival of Sonic Hedgehog-Induced Medulloblastomas

Andrew R. Hallahan,<sup>1,2</sup> Joel I. Pritchard,<sup>1</sup> Stacey Hansen,<sup>1</sup> Mark Benson,<sup>1</sup> Jennifer Stoeck,<sup>1</sup> Beryl A. Hatton,<sup>1</sup> Thomas L. Russell,<sup>1</sup> Richard G. Ellenbogen,<sup>3</sup> Irwin D. Bernstein,<sup>1,2</sup> Phillip A. Beachy,<sup>4</sup> and James M. Olson<sup>1,2</sup>

<sup>1</sup>Clinical Research Division, Fred Hutchinson Cancer Research Center, Seattle, Washington; <sup>2</sup>Division of Pediatric Oncology and <sup>3</sup>Department of Neurosurgery, University of Washington/Children's Hospital, Seattle, Washington; and <sup>4</sup>Departments of Molecular Biology and Genetics and Howard Hughes Medical Institute, Johns Hopkins University, Baltimore, Maryland

## ABSTRACT

To develop a genetically faithful model of medulloblastoma with increased tumor incidence compared with the current best model we activated the Sonic Hedgehog (Shh) pathway by transgenically expressing a constitutively active form of *Smoothed* in mouse cerebellar granule neuron precursors (ND2:SmoA1 mice). This resulted in early cerebellar granule cell hyper-proliferation and a 48% incidence of medulloblastoma formation. Gene expression studies showed an increase in the known Shh targets *Gli1* and *Nmyc* that correlated with increasing hyperplasia and tumor formation. *Notch2* and the Notch target gene, *HES5*, were also significantly elevated in *Smoothed*-induced tumors showing that Shh pathway activation is sufficient to induce Notch pathway signaling. In human medulloblastomas reverse transcription-PCR for Shh and Notch targets revealed activation of both of these pathways in most tumors when compared with normal cerebellum. Notch pathway inhibition with soluble Delta ligand or  $\gamma$  secretase inhibitors resulted in a marked reduction of viable cell numbers in medulloblastoma cell lines and primary tumor cultures. Treatment of mice with D283 medulloblastoma xenografts with a  $\gamma$  secretase inhibitor resulted in decreased proliferation and increased apoptosis, confirming that Notch signaling contributes to human medulloblastoma proliferation and survival. Medulloblastomas in ND2:SmoA1 mice and humans have concomitant increase in Shh and Notch pathway activities, both of which contribute to tumor survival.

## INTRODUCTION

Medulloblastoma is the most common malignant brain tumor of childhood, affecting ~1:150,000 children with a peak incidence at age 5 (1). These primitive neuroectodermal tumors are believed to arise from the cerebellar granule neuron precursors that undergo massive proliferation and migration immediately after birth. Proliferation of granule neuron precursors is largely driven by the basic helix-loop-helix transcription factors in the HES family and the basic helix-loop-helix zip transcription factor, *Nmyc* (2–4). Notch signaling induces HES family members, and Sonic hedgehog (Shh) signaling induces *Gli1* and *Nmyc*. Both of these pathways converge to positively regulate *cyclin D1*, a possible primary mediator of cerebellar granule neuron precursor proliferation.

Analysis of neurodevelopmental pathways in medulloblastoma provides the foundation for new therapies that specifically block mitogenic signal transduction in these tumors (5, 6). Mutations causing increased activity of the Shh pathway have been identified in up to 20% of cases. These include inactivating mutations of *PTCH1* or

*SUFU*, genes that encode negative regulators of Shh signaling, or activating mutations of *SMO*, a gene that encodes the Shh mediator *Smoothed* (7–9). Pharmacological blockade of Shh signaling in mouse and human cell culture models of medulloblastoma results in extensive cell death (10). The Shh target *Nmyc* is elevated in many medulloblastomas (11). Mutations of *APC* and *Axin* genes activate the Wnt pathway in some medulloblastomas (12, 13). *Nmyc* or *Cmyc* amplification occurs infrequently and is associated with poor outcome (14). The Notch signaling pathway has not previously been mechanistically associated with medulloblastoma.

High-quality mouse models of medulloblastoma are required for advancement of this field. The most widely used mouse model is the *Ptc* heterozygous model generated by Goodrich *et al.* (15). This model is genetically precise, yielding a medulloblastoma phenotype in animals that have derepressed Shh signaling (16), but development of tumors is limited to 10% to 20% of the mice. The relatively low tumor incidence in this model is consistent with Gorlin's syndrome, in which <1% of patients with inactivating mutations of *PTCH1* develop medulloblastoma (17). If these mice also have homozygous loss of *p53*, there is a high incidence of medulloblastomas (18). Disruption of DNA repair (*DNA ligase IV* loss) or cell cycle regulation (*Kip1*, *Ink4c*, or *Ink4d* inactivation) in conjunction with *p53* loss also results in murine medulloblastoma (19–21). Whereas these models are informative, simultaneous mutations in these pathways are rare in human disease. An alternative approach consistent with the human disease is to activate *Smoothed*. To achieve this we developed a transgenic mouse model in which candidate oncogenic pathways can be activated primarily in cerebellar granule neuron precursors through the use of the 1-kb *NeuroD2* promoter (22). We generated eight lines of mice that express a constitutively active form of *Smoothed*, *SmoA1*. Lines expressing high levels of the transgene showed early cerebellar hyperproliferation and a high rate of medulloblastoma formation. RNA and protein studies showed increased expression of both sonic hedgehog and notch target genes. Notch and Shh pathway inhibition sharply reduced proliferation of cells from ND2:SmoA1 mice. Human tumor studies using primary and cultured cells and xenografts indicated that Notch pathway activity is important for medulloblastoma survival and that combined pathway inhibition caused more cell death than individual pathway antagonism alone.

## MATERIALS AND METHODS

**ND2:Smo Transgenic Mouse Lines.** Transgenic mice were generated on a C57BL/6 background through the Fred Hutchinson Cancer Research Center Transgenic Core and maintained in accordance with the NIH Guide for the Care and Use of Experimental Animals with approval from our Institutional Animal Care and Use Committee (IR#1457). Full-length *Smoothed* with activating point mutations, *SmoA1* (23, 24) and *SmoA2* (9), was isolated by restriction digest using *HindIII-XbaI* and ligated into pCS2+ using standard cloning techniques. A *NeuroD2* 1-kB promoter fragment with *HindIII* sites at both ends was PCR amplified from pPD46.21 (22) and inserted into pCS2SmoA1 and pCS2SmoA2. Orientation was confirmed, and the constructs were sequenced to verify the absence of unintended mutations. Fragments containing the *NeuroD2* promoter, the *SmoA1* or *SmoA2* gene, and a poly-

Received 5/24/04; revised 8/15/04; accepted 8/18/04.

**Grant support:** Damon Runyon-Lilly Clinical Investigator Award (J. M. Olson), a Burroughs Wellcome Fund Career Award in the Biomedical Sciences (J. M. Olson), the Emily Dorfman Foundation for Children (A. R. Hallahan), and the Seattle Children's Hospital and Regional Medical Center Brain Tumor Research Endowment.

The costs of publication of this article were defrayed in part by the payment of page charges. This article must therefore be hereby marked *advertisement* in accordance with 18 U.S.C. Section 1734 solely to indicate this fact.

**Note.** Supplementary data for this article can be found at Cancer Research Online (<http://cancerres.aacrjournals.org>).

**Requests for reprints:** James M. Olson, Fred Hutchinson Cancer Research Center, 1100 Fairview Ave North, D4-100, Seattle, WA 98109. E-mail [jolson@fhcrc.org](mailto:jolson@fhcrc.org).

©2004 American Association for Cancer Research.

denylic acid sequence were isolated by restriction digest (*NotI-ScaI*, 4150 bp), purified using Schleicher and Schuell columns according to the manufacturer's directions and provided to the transgenic core for zygote (E0.5 fertilized eggs) injection (22). Transgene expression was quantified on genomic DNA derived from tail or toe snips using quantitative reverse transcription-PCR (RT-PCR) with the following primers: AATCTCTGCTTTTCTGCGTTGGG (forward) and CTCGGTCATTCTCACACTTG (reverse).

**Mouse Pathology and Gene Expression Studies.** Mice were anesthetized using CO<sub>2</sub> inhalation, the cerebellum removed, and tissue snap-frozen for RNA studies or fixed in 4% paraformaldehyde for pathological examination. Tissue blocks were paraffin embedded, cut into 4- $\mu$ m sections, and then stained with Hematoxylin and Eosin using standard methods. An observer blinded to the molecular data evaluated cerebellar pathology. This was classified as normal (indistinguishable from wild-type littermates), mild to moderate hyperplasia (<50% of the cerebellum morphologically abnormal), severe hyperplasia (>50% of the cerebellum morphologically abnormal), or frank tumor (sheets of small round blue cells without identifiable cerebellar architecture). His tag staining to evaluate the localization of transgene expression to cerebellar granule cells was done on frozen sections using a Penta-His mouse IgG monoclonal antibody (1:200, Molecular Probes, Eugene, OR) and a fluorescein goat antimouse secondary (1:1,000, The Jackson Laboratory, West Grove, PA). Total RNA was extracted from mouse cerebellum using an Rneasy Lipid Tissue kit per the manufacturer's instructions (Qiagen, Valencia, CA). For microarray studies each sample was labeled according to Affymetrix's recommended protocol, hybridized to individual U74Av2 oligonucleotide arrays, and scanned according to the manufacturer's recommendations (Affymetrix) with comparison to wild-type littermate controls. Scanned image files were analyzed using MAS5.0 (Affymetrix). For quantitative real-time PCR, RNA was DNase treated and converted to cDNA using the ABI Taqman Reverse Transcription kit (Applied Biosystems, Foster City, CA). Reactions were set up using ABI SYBR green or Taqman Master Mix and run on an ABI 7000 Sequence Detection System. Specific primers for mouse *Gli1*, *Gli2*, *NMyc*, *Notch1*, *Notch2*, *HES1*, *HES5*, the *Smo* transgene, and *S16* control were used (Supplementary Data; Table 1). Data were analyzed using ABI GeneAmp SDS software. All of the conditions were run in triplicate and normalized to mouse *S16* control. The same procedure was used to measure *HES1* levels in mouse bone marrow.

**Human Tumors.** Human medulloblastoma cDNA panels were obtained from the Children's Oncology Group Brain Tumor Resource Laboratory. Demographic details are provided in the Supplemental Data (Table 2). RT-PCR was performed as described above. Specific primers for *Gli1*, *Gli2*, *Patched1*, *Patched2*, *NMyc*, *Notch1*, *Notch2*, *HES1*, and *HES5* were used (Supplementary Data; Table 3). Normalization was done with an endogenous gene control (*EEF1 $\beta$* ) that we had found previously to have minimal variance in medulloblastomas. Control brain samples were from 10 pediatric subjects (median age, 16 years; range, 11 to 18 years) who died as a result of trauma or nonmalignant disease. These were from the Maryland Brain Bank, kindly supplied by the laboratory of Dr. Gregory

Riggins (Johns Hopkins University, Baltimore, MD). Expression levels from the control samples were averaged and the result set to 1. Comparison between desmoplastic and nondesmoplastic tumors was made using a two-tailed unpaired Student's *t* test. Immunostaining for Notch1 was performed using the rat antihuman Notch antibody 18G as described previously (25).

**Cell Culture and Viability Assays.** Medulloblastoma cell lines were grown as described previously (26). As controls, BW5147 cells, demonstrated previously to be resistant to Notch pathway inhibition, were obtained from American Type Culture collection and cultured as described (27). Primary brain tumor tissue was obtained from patients undergoing surgical resection after informed consent for Children's Oncology Group protocol ACNS02B1 and processed as described previously (10). These studies had prior approval from the Institutional Review Board of the hospitals where the samples were collected. Mouse brain tumor tissue was treated in the same manner as human. Cells were incubated with Delta ligand in solution (Delta-1<sup>ext-IgG</sup>; ref. 28), control IgG, the notch antagonist *N*-[*N*-(3,5-difluorophenacetyl)-L-alanyl]-S-phenylglycine t-butyl ester (DAPT/ $\gamma$  secretase inhibitor IX, Calbiochem, San Diego, CA) or DMSO at the indicated concentrations for 48 hours and total viable cell number quantified by trypan-blue hemacytometer counts and an ATP-luciferase assay (Vialight, Cambrex Bio Science, Rockland, ME). Results were normalized to vehicle-treated control cells.

**Xenografts.** Animal experiments were performed according to the NIH Guide for the Care and Use of Experimental Animals and approved by our Institutional Animal Care and Use Committee (IR#1573). D283 mouse xenografts were established in 3-month-old NOD-SCID mice as described previously (29, 30). Once tumors were  $\geq 250$  mm<sup>3</sup> the animals were treated with daily s.c. injections of DAPT in corn oil 200 mg/kg/day as described (30). After 4 days of treatment the animals were pulsed with bromodeoxyuridine (Roche Diagnostics, Indianapolis, IN) 50 mg/kg 1 hour before sacrifice, euthanized, tumors removed, and fixed in 4% paraformaldehyde overnight then embedded in paraffin. Bone marrow was removed at the time of sacrifice and *HES1* mRNA level quantified by RT-PCR as described above. Tissue sections, 4  $\mu$ m, were cut. Bromodeoxyuridine staining was performed using goat antibromodeoxyuridine antibody (Accurate Chemicals, Westbury, NY) as described (31). Apoptosis was quantified by terminal deoxynucleotidyl transferase-mediated nick end labeling staining (In Situ Cell Death Detection kit, Fluorescein, Roche Diagnostics, Mannheim, Germany). Nuclei were stained with 4',6-diamidino-2-phenylindole. An observer blinded to the treatment conditions counted at least 10 randomly selected high-powered fields per section (500 to 1,000 cells per field). Comparison between control and treatment groups was made using a two-tailed unpaired Student's *t* test.

## RESULTS

**Activation of the Sonic Hedgehog Pathway in Mouse Cerebellar Granule Neuron Precursors Results in Hyperproliferation and Medulloblastoma Formation.** To selectively activate the Shh pathway in cerebellar granule neuron precursors we expressed constitutively active forms of the Smoothed gene, *SmoA1* or *SmoA2* (24), using the NeuroD2 1-kb promoter that is principally expressed in cerebellar granule neuron precursors (Fig. 1A). Generation of the ND2:*SmoA1* lines was complicated by premature death due to tumor formation in several founder mice that had high *Smo* levels (Table 1). Three lines of mice with varying levels of *SmoA1* expression were established and observed over 12 months. Staining for the His tag expressed by the transgene confirmed selective expression in cerebellar granule cells (Fig. 1B). Forty-eight percent of the high-expressing line developed symptomatic medulloblastomas at a median age of 25.7 weeks (Fig. 1, C and D; Table 1; Supplemental Data Fig. 1). Rapid progression resulted in symptoms requiring animal sacrifice within 1 to 14 days of onset. Lines with lower levels of transgene expression did not develop tumors. The four ND2:*SmoA2* lines had relatively low levels of *Smo* expression and rarely developed tumors. To evaluate the events preceding tumor formation cohorts of ND2:*SmoA1* mice were sacrificed at 8 weeks of age and their cerebellar pathology

Table 1 ND2:*Smo* mouse lines and phenotypes

Smoothed line	Average transgene expression level (relative to WT)	Phenotype	No. of mice observed >12 mo.
SmoA1:199	30	48% tumor incidence rate	102
SmoA1:193	45	Founder developed tumor at 7 weeks (no progeny)	NA
SmoA1:232	ND	Founder developed tumor at 6 months (no progeny)	NA
SmoA1:234	36	Founder developed tumor at 3.5 months (no progeny)	NA
SmoA1:235	ND	Founder developed tumor at 8 weeks (no progeny)	NA
SmoA1:252	ND	No tumor development (no progeny)	NA
SmoA1:255	2	No tumor development	30
SmoA1:201	3	No tumor development	29
SmoA2:221	4	4 tumors observed	19
SmoA2:222	1	No tumor development	31
SmoA2:225	3	No tumor development; some hyperplasia	26
SmoA2:242	2	No tumor development	12

Abbreviations: WT, wild-type; ND, not determined; NA, not applicable.

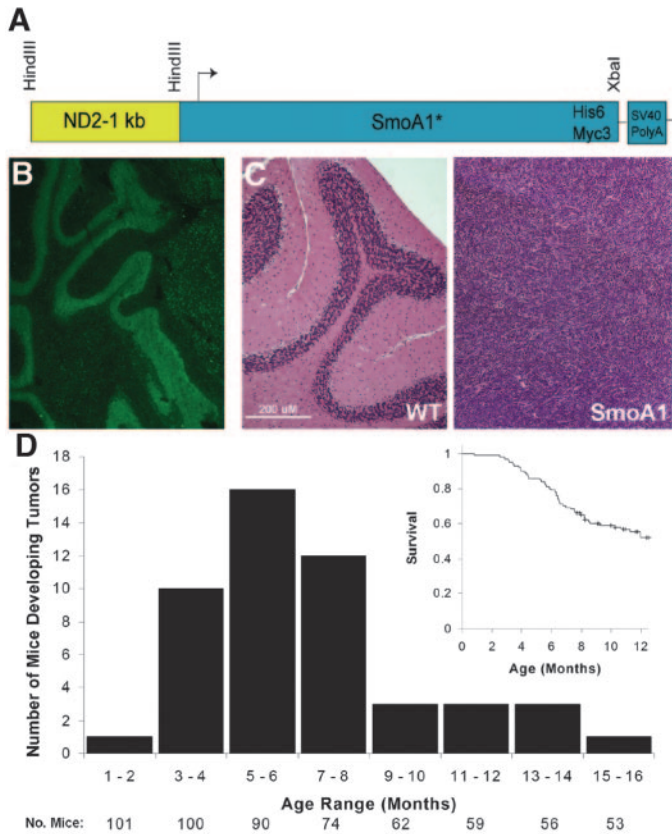


Fig. 1. ND2:SmoA1 transgenic mouse model of medulloblastoma. *A*, schematic of transgenic construct showing 1-kb portion of ND2 promoter driving expression of *SmoA1*. *SmoA1* was tagged with both *His6* and *Myc3* and contained an activating mutation as described (24). *B*, transgene expression visualized by immunofluorescent staining for the His tag in the cerebellum of an adult mouse. *C*, Hematoxylin & Eosin stained horizontal sections showing normal cerebellum in a wild-type and tumor in a ND2:SmoA1 mouse, age 2 months; scale bar = 200  $\mu$ m. *D*, observed mortality for the SmoA1:199 mouse line. The total number of mice observed in each time period is given below. The Kaplan-Meier survival curve for this cohort of mice is shown in the inset. Death in all cases was as a result of cerebellar tumor formation. (ND2, neuroD2; SmoA1, Smoothed)

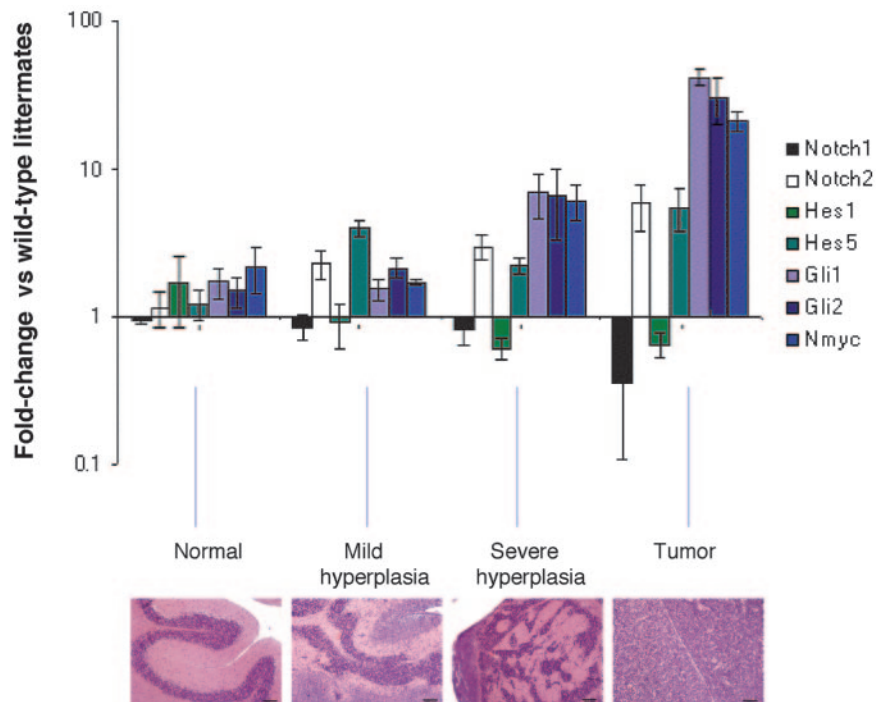
assessed. This revealed excessive granule cell proliferation in 80% of high-expressing mice (Fig. 2, histology panels). This was rarely seen in the lines of mice with low levels of *Smo* expression.

**Changes in Cerebellar Granule Neuron Precursor Mitogenic Signal Pathway Activity with Increasing Hyperplasia and Medulloblastoma Formation in ND2:SmoA1 Mice.** To elucidate the signal transduction pathways underlying cerebellar granule neuron precursor hyperplasia and tumor formation we assayed RNA expression using oligonucleotide arrays (Supplemental Data Fig. 2). A total of 3.9% (486 of 12,488) of genes had increased mRNA expression, and 3.5% (438 of 12,488) were decreased ( $P \leq 0.01$ ). As expected, there was an increase in known Shh pathway target genes including *Nmyc* and multiple cell cycle regulatory proteins. Increased expression of ribosomal proteins was also prominent, consistent with a previous human medulloblastoma gene expression study (32). An unexpected change, however, was up-regulation of *HES5*, the main Notch target gene in the developing cerebellum. *HES1* was not altered, and *HES2* was not present on the arrays (data not shown).

Given these findings, focused studies correlating pathological changes and expression of Shh and Notch pathway genes using quantitative RT-PCR were done (Fig. 2). This showed that increasing hyperplasia was associated with a progressive increase in *Nmyc*, *Gli1*, and *Gli2* with tumors having extremely high expression levels of these genes. In a similar fashion *Notch2* and *HES5* were elevated in hyperplastic cerebellum and most tumors. *HES2*, undetectable in wild-type mice, was also detectable in three of the five tumors tested (data not shown).

**Sonic Hedgehog and Notch Signaling in Human Medulloblastomas.** To determine the relevance of the above findings to human disease we assayed the expression of Shh and Notch pathway genes by RT-PCR in a panel of 24 human medulloblastomas. RNA from the normal cerebellum of 10 pediatric subjects who had died of trauma or nonmalignant disease was used as controls. Tumor pathology and clinical data were collected and are graphically represented in Figs. 3 and 4 (demographic information summarized in Supplemental Table 2). Gene expression was considered elevated if increased 2-fold or

Fig. 2. Sonic hedgehog and Notch gene expression changes in the ND2:SmoA1 mouse cerebellum. Quantitative real-time PCR was set up using ABI SYBR green Master Mix and run on an ABI 7000 Sequence Detection System. Specific primers for mouse *Notch1*, *Notch2*, *HES1*, *HES5*, *Gli1*, *Gli2*, *NMyc*, and *S16* control were used. SYBR green dye intensity was analyzed using SDS software. All conditions were run in triplicate. Each sample was amplified in triplicate and normalized to mouse S16 control. Gene expression was correlated with the cerebellar histology of the high-expressing ND2:SmoA1 mice: normal cerebellar histology indistinguishable from wild-type ( $n = 3$ ); mild hyperplasia (<50% cerebellum abnormal,  $n = 3$ ); severe hyperplasia (>50% cerebellum abnormal,  $n = 7$ ); cerebellar tumors ( $n = 7$ ). Average fold-change versus wild-type littermates is shown; bars  $\pm$ SE. Representative tissue sections are shown below; scale bars are 100  $\mu$ m.



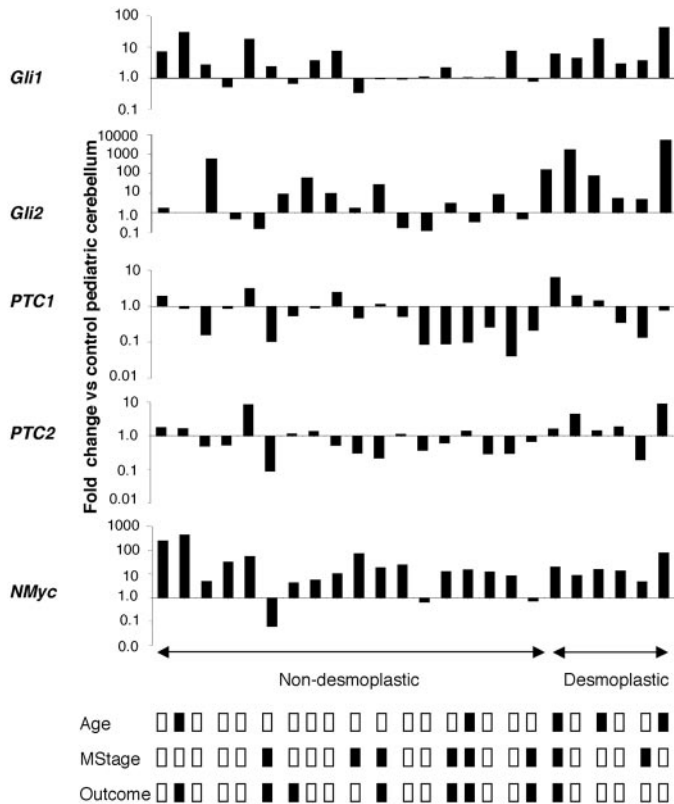


Fig. 3. Sonic hedgehog and pathway gene expression in human medulloblastomas. Quantitative RT-PCR using Sybr Green fluorescence was used to measure gene expression. Normalization was done with an endogenous gene control (*EEF1B2*) that was confirmed to not change in these samples. Normal cerebellum from 10 children without cancer was averaged and the result set to 1. Medulloblastoma samples are subdivided into desmoplastic and nondesmoplastic pathologies. Clinical data are summarized below: ■ = age < 3 years, metastatic disease present at diagnosis, died of disease. The numbers on the Y axis represent the fold change of mRNA copies of each medulloblastoma sample relative to the average of the control samples.

more above controls. Analysis revealed a widespread increase in Shh pathway activity (Fig. 3). *Gli1*, a well-validated Shh target gene (33) was elevated in 63% (15 of 24) of tumors including all of the desmoplastic cases. Notably, 50% (9 of 18) of nondesmoplastic medulloblastomas had elevated *Gli1*, indicating that Shh pathway activation is much more common in these tumors than suspected previously. *Gli2* was also elevated in all of the desmoplastic and 39% (7 of 18) nondesmoplastic tumors. Desmoplastic tumors had a statistically greater elevation of *Gli2* expression than nondesmoplastic cases ( $P = 0.04$ ). Levels of *Gli1* expression trended higher in desmoplastic versus nondesmoplastic tumors, but this did not reach statistical significance ( $P = 0.1$ ). *NMyc*, a direct target of Shh in cerebellar GNPs was elevated 88% (21 of 24) of medulloblastomas. Increased *Ptch1* expression was less frequent, present in 33% (2 of 6) of desmoplastic and 11% (2 of 18) of nondesmoplastic tumors, respectively. *Ptch2* expression paralleled that of *Ptch1*.

Focusing on the Notch pathway we found the vast majority (92%, 22 of 24) of tumors had increased notch target gene expression with elevation of either *HES1* (46%, 11 of 24) and/or *HES5* (71%, 17 of 24) mRNA levels (Fig. 4). *Notch1* was increased in 75% (18 of 24) of tumors, whereas *Notch2* was overexpressed in only 12.5% of tumors (3 of 24). No significant differences were evident between desmoplastic and nondesmoplastic tumors. Immunostaining on 7 tumors revealed that all were positive for intracellular *Notch1* at levels comparable with bone marrow (Fig. 5, A–D). Four control pediatric cerebellums were negative for Notch1 protein expression by immunocytochemistry (Fig. 5C). Transient transfections with intracellular

*Notch1* and *Notch2* plasmids confirmed the specificity of the Notch1 antibody as has been shown previously (25).

**Notch Signaling Contributes to Medulloblastoma Growth and Survival.** To ascertain if Notch pathway activity was important for medulloblastoma cell survival we added soluble Delta ligand to cultures of 2 medulloblastoma cell lines. Delta unattached to a surface acts in a dominant-negative manner (28). This resulted in 2-fold decrease in *HES1* expression in both cell lines within 7 hours and a dose-dependent decrease in viable cell number by 48 hours (Fig. 6A). We pharmacologically inhibited Notch cleavage with the  $\gamma$ -secretase inhibitor, DAPT (Calbiochem; ref. 34). In the four medulloblastoma cell lines tested this also caused a dose-dependent decrease in the number of viable cells within 48 hours of treatment (Fig. 6B). Similar effects were also seen with an alternative  $\gamma$  secretase inhibitor, L-685,458 (Calbiochem, data not shown). To control for nonpathway-specific drug effects we added DAPT to BW5147 cells, which are known to be insensitive to Notch pathway inhibition (27): this did not decrease viable cell numbers over a concentration range of 0.1 to 10.0  $\mu\text{mol/L}$ . Primary tumors from mice and humans (Fig. 6C) also had decreases in total viable cell number in response to notch pathway inhibition. The combination of Shh antagonism with cyclopamine and Notch antagonism resulted in a significantly greater response than the use of either agent alone. Short-term treatment of mice with D283 xenografts using DAPT resulted in suppression of *HES1* expression in the marrow, markedly decreased tumor cell proliferation, and significantly increased apoptosis (Fig. 6D). A 4-week study of the activity of DAPT on D283 xenografts was inconclusive, because

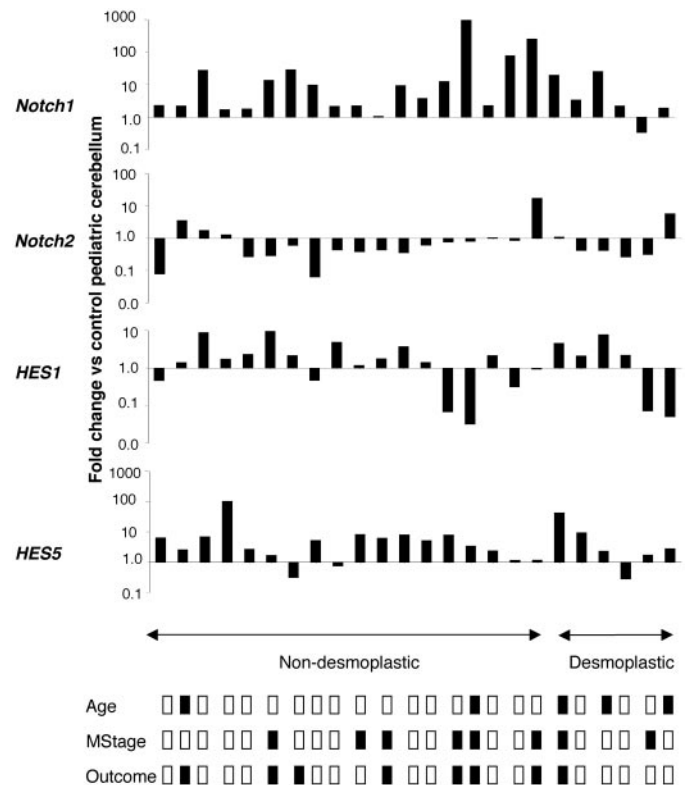
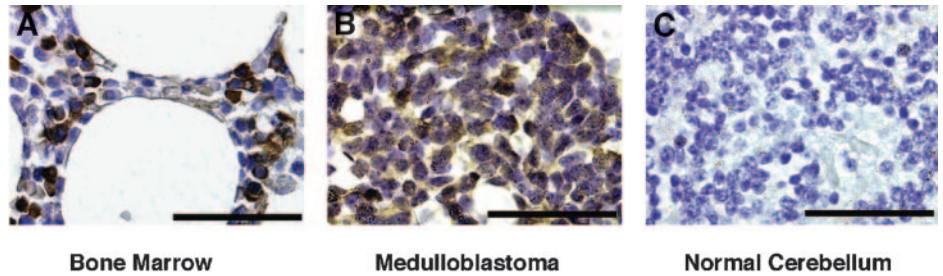


Fig. 4. Notch pathway gene expression in human medulloblastomas. Quantitative RT-PCR using Sybr Green fluorescence was used to measure gene expression. Normalization was done with an endogenous gene control (*EEF1B2*) that was confirmed to not change in these samples. Normal cerebellum from 10 children without cancer was averaged and the result set to 1. Medulloblastoma samples are subdivided into classic and desmoplastic pathology. Clinical data are summarized below: ■ = age < 3 years, metastatic disease present at diagnosis, died of disease. The numbers on the Y axis represent the fold change of mRNA copies of each medulloblastoma sample relative to the average of the control samples.

Fig. 5. Intracellular Notch1 expression in medulloblastoma. *A*, normal bone marrow stained with anti-intracellular Notch1 antibody. Positive staining is brown-black, and the counterstain is a light blue hematoxylin. Scale bar = 25  $\mu$ m. *B*, representative medulloblastoma demonstrating expression of intracellular Notch1. *C*, normal pediatric cerebellum stained with anti-intracellular Notch1 antibody.



the drug was not effective in inhibiting Notch pathway activity after 2 weeks as evidenced by failure to suppress *HES-1* expression in the marrow (data not shown).

## DISCUSSION

Our initial goal in this study was to develop a genetically faithful mouse model of medulloblastoma that would be tractable for studies of disease pathogenesis and therapeutics. Genomic studies on this model confirmed known Shh target genes along with an unexpected increase in Notch signaling, confirmed by quantitative RT-PCR. Evaluating these pathways in human tumors, we found elevated Notch and

Shh activity in most medulloblastomas. Notch inhibition with soluble Delta ligand or  $\gamma$  secretase inhibitors resulted in decreased proliferation and increased apoptosis. Whereas the mechanism of Notch activation remains to be elucidated, the consequence of the Shh pathway driving proliferation and the Notch pathway inhibiting differentiation appears critical for tumor growth.

Focusing on the Shh pathway, targeted activation of *Smoothed* in cerebellar granule neuron precursors was sufficient to cause tumors in 48% of high-expressing mice by a median 6 months of age. Importantly, preceding hyperproliferation was evident by 8 weeks of age in the majority of ND2:SmoA1 mice, providing an opportunity to study disease progression from its early stages and test

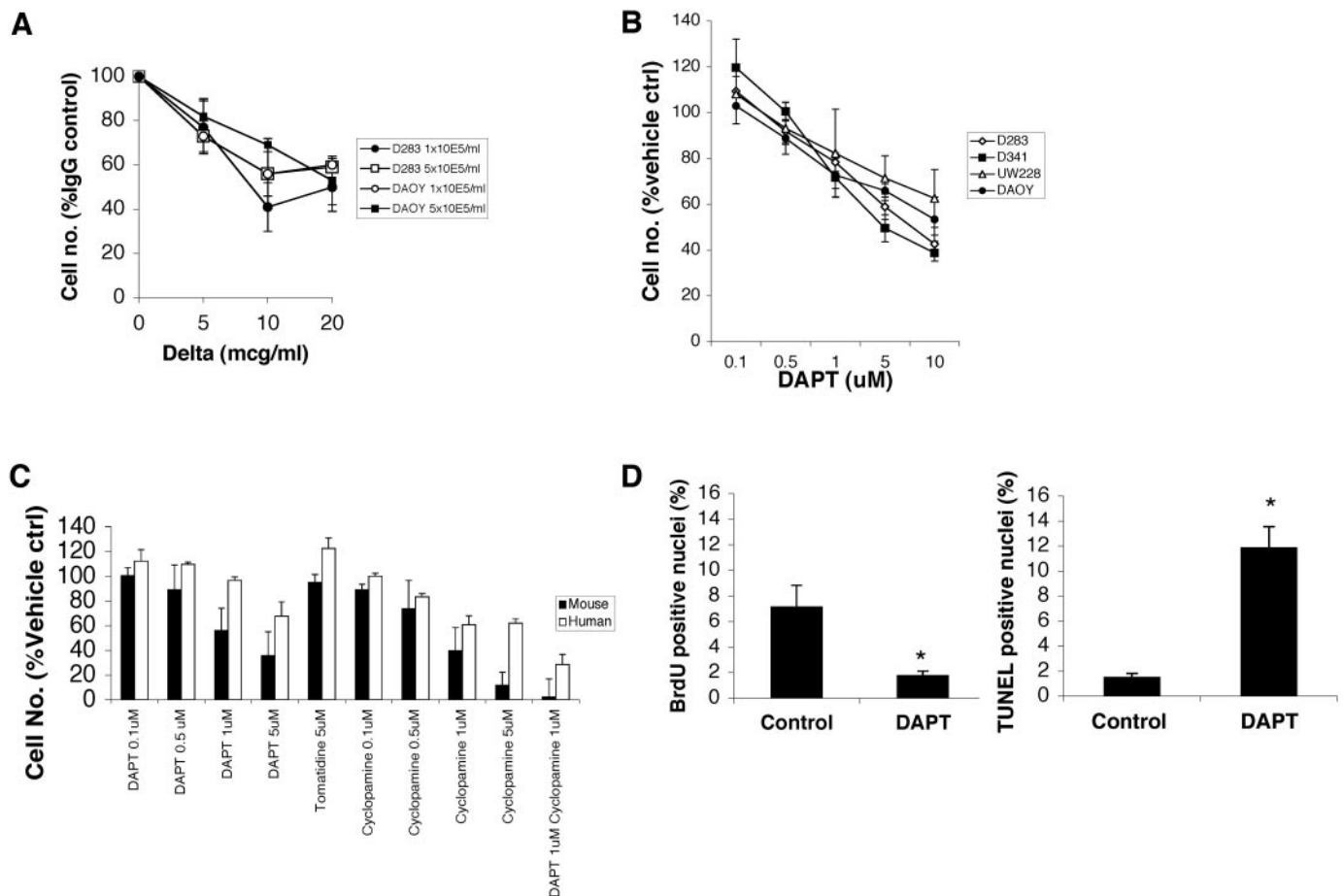


Fig. 6. Inhibition of Notch pathway activity in medulloblastoma. *A*, D283 and DAOY medulloblastoma cells were incubated with Delta-1<sup>ext-IgG</sup> in solution at the indicated concentrations for 48 hours and total viable cell number quantified by trypan blue hemacytometer counts. Results were normalized to IgG treated control cells. Data are the mean of three independent experiments; bars,  $\pm$ SE. *B*, medulloblastoma cell lines were incubated with the notch antagonist DAPT at the indicated concentrations for 48 hours and total cell number quantified by an ATP-luciferase assay. Results were normalized to vehicle-treated control cells. Data shown is the mean of three independent experiments. *C*, ND2:SmoA1 mouse and human primary medulloblastoma treated immediately after removal with antagonism of Notch (DAPT), Shh (cyclopamine), or the combination of these. Cell number relative to vehicle treated control was measured as in *B* at 48 hours. Data are the mean of three independent measurements in a representative tumor; bars,  $\pm$ SE. *D*, treatment of D283 xenografts in NOD-SCID mice with DAPT 200 mg/kg/day for 4 days resulted in significantly decreased proliferation and increased apoptosis of tumor cells. Data are the mean from three independent tumors, bars,  $\pm$ SE; \*,  $P < 0.05$ .

novel approaches to treatment. ND2:SmoA1 lines with low levels of transgene expression had no phenotype, confirming that high levels of activated *Smoothed* are required for Shh pathway activation, consistent with the studies of Lum *et al.* (35) in *Drosophila*. Even among mice in the high expressing line, there was a small subset that did not show elevation of *Nmyc*, *Gli*, or *Notch* pathway components and had a normal histologic phenotype. The ND2:SmoA1 model is, thus, the only mouse model of medulloblastoma with early pathology and a high incidence of tumors that does not have loss of *p53* or other genetic mutations that are uncommon in human medulloblastomas.

In human medulloblastomas increased Shh signaling has been described in desmoplastic tumors (32). A limitation with prior studies of neurodevelopmental pathways in human medulloblastoma samples has been lack of an appropriate comparison group of normal pediatric cerebellum. By addressing this we found that Shh pathway activation is common in classic medulloblastomas as well as desmoplastic tumors. This is consistent with the extensive cell death induced in classic medulloblastomas when the Shh pathway is inhibited (10). *Ptc1* and *Ptc2*, key Shh pathway regulators, were elevated in a minority of tumors despite increased *Gli1* and *Gli2*, indicating aberrant regulation of this negative feedback loop in medulloblastomas.

The events cooperating with Shh signaling in human tumor genesis and growth have not been defined. Notch signaling both inhibits differentiation and promotes proliferation in the developing cerebellum (2). The findings in the ND2:SmoA1 mouse prompted evaluation of Notch signaling in human medulloblastomas. *Notch1* mRNA was increased in 75% of human tumors, and *Notch2* mRNA was increased in 12% of cases. The Notch target genes *HES5* and *HES1* were increased in 92% of tumors. A recent study using suppression subtractive hybridization found an increase in *Mushashi-1*, a negative regulator of the Notch antagonist *Numb* in medulloblastomas (36). A change in *Numb* levels was not found, and elevated Notch pathway activity was only demonstrated in the TE671 cell line. Colleagues in another laboratory have found that *Notch2* is increased more frequently than *Notch1* in human medulloblastoma.<sup>5</sup> To assess the validity of our RT-PCR data for Notch1, we evaluated Notch1 protein expression in human tumors by immunocytochemistry using an antibody that we confirmed to be specific for Notch1. All 7 of the cases evaluated showed Notch1 protein expression comparable with that seen in bone marrow. In most cases, the staining showed a nuclear pattern, consistent with cleaved intracellular Notch. Control pediatric cerebellum was negative for Notch 1. In both *Notch1*- and *Notch2*-positive medulloblastomas, *HES5* expression is increased, suggesting that this may be a mediator of oncogenic Notch pathway signals in both ND2:SmoA1 mice and human medulloblastoma patients. However, the Notch pathway has multiple downstream mechanisms of activity, and detailed mouse genetic studies are necessary to define which are critical for medulloblastoma genesis and growth.

Notch and Shh have a complex pattern of overlapping expression and regulation in development, and each is recognized as an oncogene in a variety of cancers (37–39). Notch has been implicated in the pathogenesis of Hodgkin's disease and large-cell anaplastic lymphomas and is an oncogene in T-cell lymphoma (40, 41). In breast cancer cell lines Notch signaling has been demonstrated to maintain the phenotype of ras-transformed cells (42). Overexpression of Notch receptors is well described in cervical carcinoma and has been linked to human papillomavirus E6 and E7 proteins (43). Recently, aberrant Notch activity has been shown in pancreatic cancer (44). It is notable that separate studies have implicated abnormal persistent Shh activity

in pancreatic cancer as well (45), but coexpression and interactions of these pathways have not yet been investigated in these or other tumors.

Signal pathways that contribute to tumor genesis or progression often mediate the survival of tumor cells. This is clearly the case with Shh signaling in medulloblastoma, lung, and pancreatic tumors where inhibition results in significant cell death (10, 46, 47).  $\gamma$ -Secretase inhibitors target Notch signaling in tumor cells and have been shown recently to markedly decrease the growth of T-cell lymphomas (27). We found a similar response in 4 medulloblastoma cell lines with a 40% to 60% decrease in total viable cell number after 48 hours of treatment. Primary mouse and human tumors had similar responses to DAPT as well as cyclopamine, supporting the validity of the mouse model. The effect of combined Shh and Notch pathway inhibition appeared to be additive in these primary tumors. *In vivo* evaluation of Notch pathway inhibition was complicated by inability of the drug to inhibit Notch target gene expression after 2 weeks, presumably because of an increase in drug metabolism. Short-term treatment with DAPT demonstrated decreased proliferation and increased apoptosis at levels comparable with treatment with cisplatin (Hallahan A. R. and Olson J. M., unpublished data). This establishes Notch signaling as critical for the survival of medulloblastoma cells with potential as a therapeutic target.

The ND2:Smo mouse model of medulloblastoma demonstrates that Notch pathway activation occurs in Shh-induced tumors. This resulted in a re-evaluation of human medulloblastomas, which revealed that activation of both pathways is common. The prognostic significance of this is not known and requires evaluation on a large cohort of uniformly treated cases. Pharmacological antagonism of either pathway resulted in high levels of cell death (10). Combining agents that blocked both Shh and Notch activity led to rapid, near complete medulloblastoma cell death. The challenges of considering systemic Notch antagonism for cancer therapy, however, are significant. Notch signaling is critical for lymphopoiesis and probably gut regeneration, raising the possibility of a narrow therapeutic window (48). Innovative strategies will likely be based on elucidation of the critical differences between Notch activities in oncogenesis *versus* that in nonneoplastic tissue regeneration. Additional studies that elucidate the mechanisms by which the Notch and Shh pathways interact in cancer genesis and growth are indicated.

## ACKNOWLEDGMENTS

We thank Dr. Stephen Tapscott for helpful review and advice, Dr. Charles Eberhart for sharing advice, data, samples and reagents prior to publication, Dr. David Flowers and Dr. Barbara Varnum-Finney in the Bernstein laboratory for reagents and advice and Dr. Anna Bigas for intracellular Notch2 plasmids. We are grateful for provision of human tumor tissue from collaborators in the Children's Oncology Group and control pediatric cerebellar tissue from the Maryland and Harvard Brain Banks.

## REFERENCES

1. Packer RJ, Cogen P, Vezina G, Rorke LB. Medulloblastoma: clinical and biologic aspects. *Neuro-oncol* 1999;1:232–50.
2. Solecki DJ, Liu XL, Tomoda T, Fang Y, Hatten ME. Activated Notch2 signaling inhibits differentiation of cerebellar granule neuron precursors by maintaining proliferation. *Neuron* 2001;31:557–68.
3. Kenney AM, Cole MD, Rowitch DH. *Nmyc* upregulation by sonic hedgehog signaling promotes proliferation in developing cerebellar granule neuron precursors. *Development* 2003;130:15–28.
4. Oliver TG, Grasfeder LL, Carroll AL, et al. Transcriptional profiling of the Sonic hedgehog response: a critical role for N-myc in proliferation of neuronal precursors. *Proc Natl Acad Sci USA* 2003;100:7331–6.
5. Dahmane N, Sanchez P, Gitton Y, et al. The Sonic Hedgehog-Gli pathway regulates dorsal brain growth and tumorigenesis. *Development* 2001;128:5201–12.
6. Wechsler-Reya R, Scott MP. The developmental biology of brain tumors. *Annu Rev Neurosci* 2001;24:385–428.

<sup>5</sup> C. Eberhart, personal communication.

7. Vorechovsky I, Tingby O, Hartman M, et al. Somatic mutations in the human homologue of *Drosophila* patched in primitive neuroectodermal tumours. *Oncogene* 1997;15:361–6.
8. Taylor MD, Liu L, Raffel C, et al. Mutations in *SUFU* predispose to medulloblastoma. *Nat Genet* 2002;31:306–10.
9. Reifenberger J, Wolter M, Weber RG, et al. Missense mutations in *SMOH* in sporadic basal cell carcinomas of the skin and primitive neuroectodermal tumors of the central nervous system. *Cancer Res* 1998;58:1798–803.
10. Berman DM, Karhadkar SS, Hallahan AR, et al. Medulloblastoma growth inhibition by hedgehog pathway blockade. *Science* 2002;297:1559–61.
11. Grotzer MA, Hogarty MD, Janss AJ, et al. MYC messenger RNA expression predicts survival outcome in childhood primitive neuroectodermal tumor/medulloblastoma. *Clin Cancer Res* 2001;7:2425–33.
12. Dahmen RP, Koch A, Denkhaus D, et al. Deletions of *AXIN1*, a component of the WNT/wingless pathway, in sporadic medulloblastomas. *Cancer Res* 2001;61:7039–43.
13. Huang H, Mahler-Araujo BM, Sankila A, et al. APC mutations in sporadic medulloblastomas. *Am J Pathol* 2000;156:433–7.
14. Aldosari N, Bigner SH, Burger PC, et al. MYCC and MYCN oncogene amplification in medulloblastoma. A fluorescence in situ hybridization study on paraffin sections from the Children's Oncology Group. *Arch Pathol Lab Med* 2002;126:540–4.
15. Goodrich LV, Milenkovic L, Higgins KM, Scott MP. Altered neural cell fates and medulloblastoma in mouse patched mutants. *Science* 1997;277:1109–13.
16. Kim JY, Nelson AL, Algon SA, et al. Medulloblastoma tumorigenesis diverges from cerebellar granule cell differentiation in patched heterozygous mice. *Dev Biol* 2003;263:50–66.
17. Cowan R, Hoban P, Kelsey A, Birch JM, Gattamaneni R, Evans DG. The gene for the naevoid basal cell carcinoma syndrome acts as a tumour-suppressor gene in medulloblastoma. *Br J Cancer* 1997;76:141–5.
18. Wetmore C, Eberhart DE, Curran T. Loss of p53 but not ARF accelerates medulloblastoma in mice heterozygous for patched. *Cancer Res* 2001;61:513–6.
19. Lee Y, Miller HL, Jensen P, et al. A molecular fingerprint for medulloblastoma. *Cancer Res* 2003;63:5428–37.
20. Zindy F, Nilsson LM, Nguyen L, et al. Hemangiosarcomas, medulloblastomas, and other tumors in *Ink4c/p53*-null mice. *Cancer Res* 2003;63:5420–7.
21. Lee Y, McKinnon PJ. DNA ligase IV suppresses medulloblastoma formation. *Cancer Res* 2002;62:6395–9.
22. Lin CH, Stoeck J, Ravanpay AC, Guillemot F, Tapscott SJ, Olson JM. Regulation of neuroD2 expression in mouse brain. *Dev Biol* 2004;265:234–45.
23. Xie J, Murone M, Luoh SM, et al. Activating Smoothed mutations in sporadic basal-cell carcinoma. *Nature (Lond)* 1998;391:90–92.
24. Taipale J, Chen JK, Cooper MK, et al. Effects of oncogenic mutations in Smoothed and Patched can be reversed by cyclopamine. *Nature* 2000;406:1005–9.
25. Ohishi K, Varnum-Finney B, Serda RE, Anasetti C, Bernstein ID. The Notch ligand, Delta-1, inhibits the differentiation of monocytes into macrophages but permits their differentiation into dendritic cells. *Blood* 2001;98:1402–7.
26. Rostomily RC, Birmingham-McDonogh O, Berger MS, Tapscott SJ, Reh TA, Olson JM. Expression of neurogenic basic helix-loop-helix genes in primitive neuroectodermal tumors. *Cancer Res* 1997;57:3526–31.
27. Weng AP, Nam Y, Wolfe MS, et al. Growth suppression of pre-T acute lymphoblastic leukemia cells by inhibition of notch signaling. *Mol Cell Biol* 2003;23:655–64.
28. Varnum-Finney B, Wu L, Yu M, et al. Immobilization of Notch ligand, Delta-1, is required for induction of notch signaling. *J Cell Sci* 2000;113 Pt 23:4313–8.
29. Hallahan AR, Pritchard JI, Chandraratna RA, et al. BMP-2 mediates retinoid-induced apoptosis in medulloblastoma cells through a paracrine effect. *Nat Med* 2003;9:1033–8.
30. Dovey HF, John V, Anderson JP, et al. Functional gamma-secretase inhibitors reduce beta-amyloid peptide levels in brain. *J Neurochem* 2001;76:173–81.
31. Monje ML, Mizumatsu S, Fike JR, Palmer TD. Irradiation induces neural precursor-cell dysfunction. *Nat Med* 2002;8:955–62.
32. Pomeroy SL, Tamayo P, Gaasenbeek M, et al. Prediction of central nervous system embryonal tumour outcome based on gene expression. *Nature* 2002;415:436–42.
33. Lee J, Platt KA, Censullo P, Ruiz I, Altaba A. Gli1 is a target of Sonic hedgehog that induces ventral neural tube development. *Development* 1997;124:2537–52.
34. Geling A, Steiner H, Willem M, Bally-Cuif L, Haass C. A gamma-secretase inhibitor blocks Notch signaling in vivo and causes a severe neurogenic phenotype in zebrafish. *EMBO Rep* 2002;3:688–94.
35. Lum L, Zhang C, Oh S, et al. Hedgehog signal transduction via Smoothed association with a cytoplasmic complex scaffolded by the atypical kinesin, Costal-2. *Mol Cell* 2003;12:1261–74.
36. Yokota N, Mainprize TG, Taylor MD, et al. Identification of differentially expressed and developmentally regulated genes in medulloblastoma using suppression subtraction hybridization. *Oncogene* 2004;23:3444–53.
37. Allenspach EJ, Maillard I, Aster JC, Pear WS. Notch signaling in cancer. *Cancer Biol Ther* 2002;1:466–76.
38. Taipale J, Beachy PA. The Hedgehog and Wnt signalling pathways in cancer. *Nature* 2001;411:349–54.
39. Radtke F, Raj K. The role of Notch in tumorigenesis: oncogene or tumour suppressor? *Nat Rev Cancer* 2003;3:756–67.
40. Jundt F, Anagnostopoulos I, Forster R, Mathas S, Stein H, Dorken B. Activated Notch1 signaling promotes tumor cell proliferation and survival in Hodgkin and anaplastic large cell lymphoma. *Blood* 2002;99:3398–403.
41. Pear WS, Aster JC, Scott ML, et al. Exclusive development of T cell neoplasms in mice transplanted with bone marrow expressing activated Notch alleles. *J Exp Med* 1996;183:2283–91.
42. Weijnen S, Rizzo P, Braid M, et al. Activation of Notch-1 signaling maintains the neoplastic phenotype in human Ras-transformed cells. *Nat Med* 2002;8:979–86.
43. Weijnen S, Zlobin A, Braid M, Miele L, Kast WM. HPV16 E6 and E7 oncoproteins regulate Notch-1 expression and cooperate to induce transformation. *J Cell Physiol* 2003;194:356–62.
44. Miyamoto Y, Maitra A, Ghosh B, et al. Notch mediates TGF alpha-induced changes in epithelial differentiation during pancreatic tumorigenesis. *Cancer Cell* 2003;3:565–76.
45. Thayer SP, di Magliano MP, Heiser PW, et al. Hedgehog is an early and late mediator of pancreatic cancer tumorigenesis. *Nature (Lond)* 2003;425:851–6.
46. Berman DM, Karhadkar SS, Maitra A, et al. Widespread requirement for Hedgehog ligand stimulation in growth of digestive tract tumours. *Nature* 2003;425:846–51.
47. Watkins DN, Berman DM, Burkholder SG, Wang B, Beachy PA, Baylin SB. Hedgehog signalling within airway epithelial progenitors and in small-cell lung cancer. *Nature (Lond)* 2003;422:313–7.
48. Wong GT, Manfra D, Poulet FM, et al. Chronic treatment with the gamma-secretase inhibitor LY-411,575 inhibits beta-amyloid peptide production and alters lymphopoiesis and intestinal cell differentiation. *J Biol Chem* 2004;279:12876–82.